AIAA AVIATION Forum
June 25-29, 2018, Atlanta, Georgia
2018 Applied Aerodynamics Conference

10.2514/6.2018-3642

Submitted to AIAA Aviation 2018, 25-29 June, Atlanta, Georgia

Swiss/Finnish Collaboration on Aeroelastic Simulations for the F/A-18 Fighter

J.B. Vos*, D. Charbonnier†,
CFS Engineering, EPFL Innovation Park, Batiment A, CH-1015 Lausanne, Switzerland
T. Siikonen‡, E. Salminen§,
Elomatic Ltd, Vaisalantie 2, FI-02130 Espoo, Finland
J. Hoffren¶,
Patria Aviation Ltd, Hatanpään valtatie 30, FI-33100 Tampere, Finland
*A. Gehri‖, P. Stephani**,*
RUAG Aviation, Aerodynamics Department, CH-6032, Emmen, Switzerland

In this paper aeroelastic simulations are presented for the F/A-18 fighter. Two CFD solvers (NSMB and FINFLO) developed in two countries, two computational grids and FEM models are utilized. In addition, different turbulence closures are applied. Results are given for a deformed and undeformed geometries by varying turbulence models, grid densities and the computational grids.

I. Introduction

The Swiss and Finnish Airforces are operating the F/A-18 C/D aircraft since 1995. Both countries invested in Computational Fluid Dynamics (CFD) tools to support the engineering and maintenance of this aircraft and in particular its structural integrity. RUAG/CFS employ and develop the NSMB CFD solver [1], while Finflo employs and develops the FINFLO CFD solver. Finflo became part of Elomatic Ltd. in September 2017.

In 2005 a first meeting was organized between RUAG/CFS from Switzerland and Finflo Ltd from Finland to exchange experiences on CFD technology, and in particular concerning the F/A-18 fighter simulations. The objective was to improve solver technology and grids in order to reduce the uncertainty in the simulation results. Different F/A-18 test cases were defined and simulated using both CFD solvers. Grids were exchanged to assess differences in simulation results that can be attributed to different grids. In 2010 load cases from the Finnish loads monitoring program (MINIHOLM) were selected for CFD simulation using both NSMB and FINFLO. From the CFD results component loads were extracted and compared, showing only small differences in loads obtained using the two CFD solvers.

CFD solver developments and grids have considerably improved since the start of the Swiss-Finnish collaboration in 2005. The second generation grid used for the F/A-18 simulations in 2005 had about 14 Million grids points (half configuration), while the third generation grids in use since 2012 (Switzerland) and 2010 (Finland) have about 50 Million points depending on the configuration [2]. In 2005 calculations were made for a rigid aircraft, today F/A-18 calculations are made on a routine base for a flexible aircraft [3] taking into account the deformation of the aircraft by the aerodynamic loads. On the Swiss side a flexible coupling tool has been compiled between NSMB and the B2000++ [4] FEM package. FINFLO has been applied with the MSC Nastran code [5]. The coupling between the CFD and FEM solutions is made utilizing in-house software tailored for the F/A-18 geometry.

In the following the main features of the flow solvers as well as the B2000++ software are described. Next the basic features of the flow solution applied in this study are shortly reviewed. The CFD-CSM coupling tool and the aeroelastic

*Director, jan.vos@cfse.ch, Senior AIAA member
†Senior Scientist, dominique.charbonnier@cfse.ch
‡Senior Adviser, timo.siikonen@elomatic.com, Senior AIAA member
§Design Manager, esa.salminen@elomatic.com
¶Research Engineer, jaakko.hoffren@patria.fi
‖Senior Scientist, alain.gehri@cfse.ch
**Senior Scientist, philippe.stephani@aerodynamics.ch

environment are represented in a case of NSMB coupling with B2000++. As a test case, a steady-state pull-up (W035) is utilized. Several combinations of the codes, grids and turbulence closures are applied. Finally, some conclusions are made.

II. CFD and FEM Software

A. NSMB CFD solver

The Navier Stokes Multi Block solver NSMB was initially developed in 1992 at the Swiss Federal Institute of Technology (EPFL) in Lausanne, and from 1993 onwards in the NSMB consortium composed of different universities, research establishments and industries. Today NSMB is developed by IMF-Toulouse (IMF Toulouse, France), ICUBE (Strasbourg, France), University of Munchen (TUM, Germany), University of the Army in Munchen (Germany), Airbus Safran (France), RUAG Aviation and CFS Engineering. A variety of papers have been published on NSMB, examples are in Refs.[1, 3, 6–14].

NSMB is a parallelized CFD solver employing the cell-centered finite volume method using multi block structured grids to discretize the Navier-Stokes equations. The patch grid and the Chimera grid approach are available to facilitate the grid generation for complex geometries. In addition, the Chimera method is used for simulations involving moving bodies. Various space discretization schemes are available, among them the 2^{nd} and 4^{th} order central schemes with an artificial dissipation and Roe and AUSM upwind schemes from 1^{st} to 5^{th} order. Time integration can be made using the explicit Runge-Kutta schemes, or the semi-implicit LU-SGS scheme. Various methods are available to accelerate the convergence to steady state, as for example local time stepping, multigrid and full multigrid, and low Mach number preconditioning. The dual time stepping approach is used for unsteady simulations.

In NSMB turbulence is modeled using standard approaches as for example the algebraic Baldwin-Lomax model, the one-equation Spalart model [15] (and several of its variants) and the $k-\omega$ family of models (including the Wilcox and Menter Shear Stress models). Hybrid RANS-LES models are available, and the code includes also a transition model solving transport equations [16].

NSMB includes remeshing algorithms that are employed for bow shock capturing for hypersonic flow problems, and for re-generation of the grid when the structure is deformed. The remeshing procedure is a combination of Volume Spline Interpolation (VSI) [17] and Transfinite Interpolation (TFI). When using Chimera grids, the remeshing procedure is carried out in each Chimera grid independent of the other Chimera grids.

B. FINFLO CFD solver

The development of the FINFLO flow solver started in the late 1980s at the former Helsinki University of Technology. In the early stage VTT Technical Research Centre of Finland and Lappeenranta University of Technology took part in the development projects funded by the domestic funding organisations and the Finnish Air Force. In the year 2001 Finflo Ltd took the responsibility to maintain the code.

Like NSMB, FINFLO is a parallelized CFD solver based on the same basic elements as NSMB. Several versions of the Chimera approach has been developed, since the first implementation [18]. The present approach is fully automatic, requires no hole-cutting and can be applied with moving bodies. The flaps and external stores of the F/A-18 aircraft are modelled using Chimera blocks. The Navier-Stokes equations are discretized in space as based on the MUSCL-formula that is 2^{nd} order accurate in space. Several flux limiters can be applied. The inviscid fluxes are evaluated using Roe, AUSM, Van Leer or a central scheme with an artificial dissipation. For compressible flows usually the Roe scheme is applied. FINFLO also contains a pressure-based solution method. The flux formula in that case can applied for all flow speeds [19]. For the density-based solution the time integration is based on the DDADI- or the LU-SGS-schemes. Dual-time stepping in the time-accurate cases, multigrid etc. are handled similar to the NSMB code. The pressure-based solver utilizes a Poisson equation for the pressure-velocity coupling and a segregated approach. This approach can be in principle applied for high-Mach-number flows [19], but the solution is in that case inefficient. FINFLO has been widely applied for marine applications. In the case of ship propellers the code is also applied for cavitating flows [20, 21].

Turbulence modeling includes the common two-equation models, Wallin-Johansson EARSM [22] and the one-equation Spalart-Allmaras model [15]. With the Spalart-Allmaras model the DES-variant is used in time-dependent simulations. The SST $k-\omega$ model is also the base model for the DES, DDES and SAS approaches as for the transition modeling [16].

FINFLO has been used with the MSC Nastran FEM-package for static fluid structure interaction problems. Typically,

5–10 iterations are needed to find the converged wing position. In the present study the deformations are calculated using the MSC Nastran software [5], but a coupling with the B2000++ code has also been made.

C. B2000++ FEM Solver

B2000++ is a Finite Element Method (FEM) solver developed by SMR Engineering & Development [4]. It can be used to study a variety of problems in aerospace engineering, ranging from the entire aircraft to components or sub-components such as stiffened panels. The element library includes shell elements, beam elements, point-mass elements, rigid-body elements, as well as 2D and 3D elements. Linear static analysis, linear dynamic analysis, free-vibration analysis and buckling analysis can be selected, as well as nonlinear static and dynamic analysis. For strength analysis, several failure criteria for isotropic materials and laminated composites are available.

One of the strengths of B2000++ is its high computational effectiveness. Symmetric multi-processing (SMP) accelerates the element procedures, taking advantage of today's multi-core CPU's. The open-source matrix solver MUMPS provides distributed parallelism via MPI. Eigen-analysis is carried out with the implicitly restarted Lanczos solver that is implemented in the open-source package ARPACK.

B2000++ is implemented in C++, and its modular architecture permits adding new solution methods, new material and element formulations, new essential and natural boundary conditions with only a few modifications to the existing code. This flexibility enables the adaptation of B2000++ to specific problems like coupled fully nonlinear FSI.

III. Solution Methods

A. Flow solution

A structured grid topology is shared by NSMB as well as by FINFLO. The structured blocks can be connected arbitrary and a non-matching coupling between the blocks is used in the Swiss computational grid. Both codes utilize the Chimera method in order to improve their capabilities in handling complex geometries. The Chimera method applied is not based on hole-cutting. Instead, the background grid values are interpolated into the ghost cells of the Chimera block. Inside the Chimera block the background grid cell may dominate the solution, if its distance to the solid wall owned by the block is shorter than that in the Chimera block. The dominance criteria is automatic and based only on the calculated wall distances. There is no limit for the number of overlapping Chimera blocks, but in the case of multiple Chimera blocks, the priority of the blocks must be set in advance.

As mentioned above the codes have several possibilities for a discretization of the inviscid fluxes. In this study a central-difference approximation with artificial dissipation is applied for convection terms in NSMB. In FINFLO a second-order upwind method with the van Albada limiter [23] is applied. The viscous terms are centrally differenced and a thin-layer approximation is used.

Since the background flow solution generally may dominate inside the Chimera blocks, a fortified algorithm is applied to force the background solution into the Chimera-block cells [24]. In the fortified algorithm a source term is added on the right-hand side of the flow equations as

$$\frac{\partial \mathbf{U}}{\partial t} + \nabla \cdot \mathbf{F}(\mathbf{U}) = \chi(\mathbf{U_f} - \mathbf{U}) \tag{1}$$

where $\mathbf{U}$ is a vector of dependent variables, $\mathbf{F}$ the flux term and $\mathbf{U_f}$ the value of the solution vector interpolated from the background grid. Parameter χ is set to a non-zero large value in the cells, where the background grid dominates. For the density-based methods the conservative values for $\mathbf{U_f}$ must be used, whereas for a segregated pressure-based method primitive values as pressure and temperature can be applied. The fortified algorithm is used together with the LU-SGS method [25]. This method consists of two lateral sweeps and between the sweeps the double influence of χ caused by two sweeps is divided out. A multigrid algorithm is also applied as based on the LU-SGS method. The values of $\mathbf{U_f}$ are lumped together from the dense grid level to the coarser levels. The Chimera interpolations are not made on the coarse grid levels.

Two RANS turbulence models are applied in this study. Spalart-Allmaras [15] and Menter's SST $k-\omega$ models are widely used and validated turbulence closures in aerodynamic applications [26]. Transition is neglected although it might have some influence on the boundary layer of the flaps and on the flow in the gaps between the flaps and wings.

B. CFD-CSM coupling tool

NSMB has been coupled to the B2000++ open-source Finite Element Method (FEM) solver [4] , see [3] for details. A geometric coupling tool was developed to transfer the aerodynamic forces from the CFD wetted surface to the structural FEM model, and to transfer the computed displacements back to the CFD surface grid. The geometric coupling tool employs a multi-region spatial interpolation procedure that is particular useful for the F/A-18 aircraft. Fig. 1 shows the FEM model of the wing, control surfaces and launchers and the corresponding CFD grid, and Fig. 2 shows the coupled CSM-CFD model. The control surfaces and the launcher in the CFD grid are indicated with a different color. Since the control surfaces can move independently of the wing, they need to be treated in separate coupling regions while at the same time C^0 continuity constraints need to be enforced at the coupling region intersections. This procedure preserves the total force and optionally the total moment, and it is energy-conservative, which is important in flutter analysis. The deformed CFD surface is smooth except at the coupling region intersections.

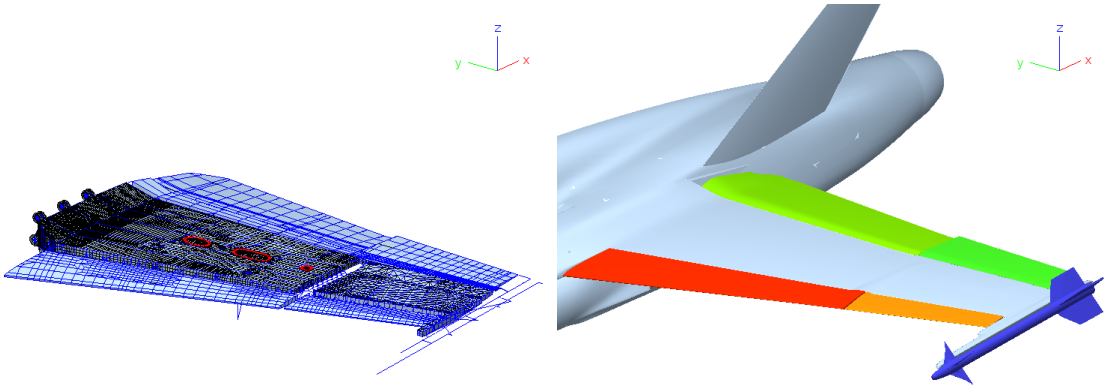

Fig. 1 CSM grid (left) and CFD grid (right) of the F/A-18 wing.

The creation of the coupling regions is done through the interactive and graphical tool FSCON (Fluid-Structure CONnector). FSCON allows selecting and visualize individual parts of the CFD wetted surface and of the FEM model. For the CFD model, boundary condition codes are used to select the coupling regions, whereas nodesets, elementsets, group codes, etc. are used for the FEM model. Thus, the coupling region definitions are independent of the mesh size and aircraft configuration. Coupling the Finnish CFD model to the FEM model used here was an effort that took only a few minutes, despite the fact that the Finnish and Swiss CFD model are totally different.

C. Aeroelastic Simulation Environment

The development of the aeroelastic simulation environment started in 2005 [27], and consists in the current state of development of the following components:

- a CFD solver using the ALE formulation that includes a remeshing algorithm;
- an interactive graphical tool to set-up the spatial coupling;
- a FEM solver to compute the structural state and to carry out the spatial coupling;
- a spatial coupling tool that can be utilized independently of the FEM solver.

The FEM and CFD solvers communicate via the Message Passing Interface (MPI), on top of which a high-level communication protocol has been implemented for structured data encapsulation. Both solvers are launched at the same time through the `mpiexec` command:

```
mpiexec -np 4 cfdsolver :  -np 1 b2000++ -mpi-sleep 1
```

The CFD solver controls the time step and the time increment size. The spatial coupling is implemented in the B2000++ FEM solver. Due to the modular architecture, integration of other CFD codes is simplified as only the MPI communication interface needs to be adapted.

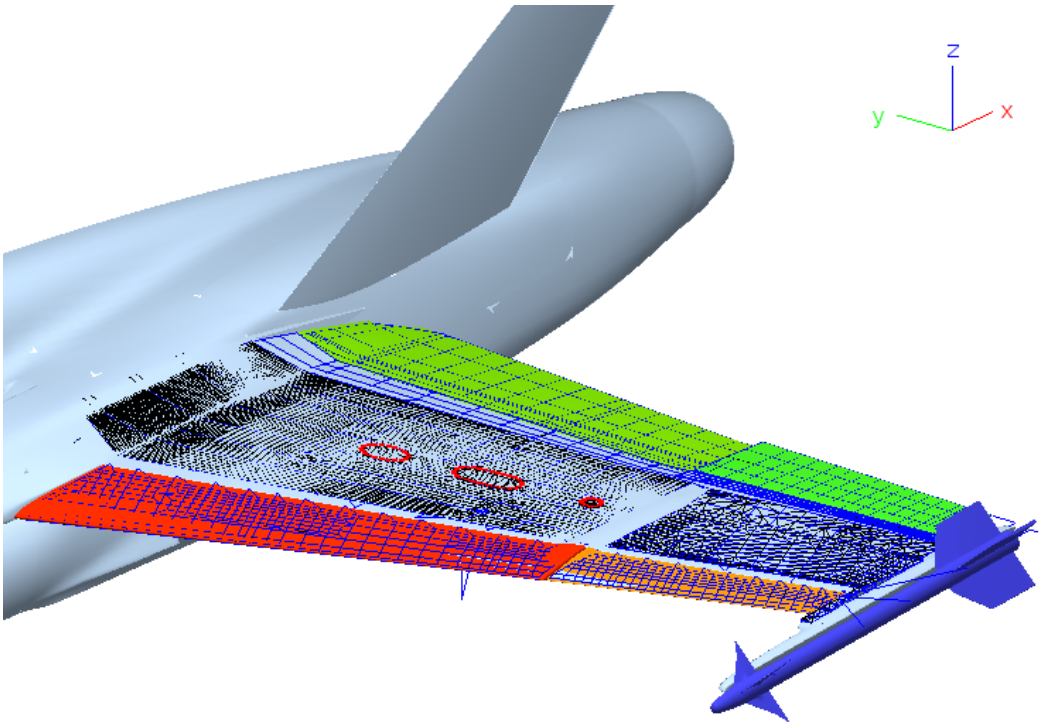

Fig. 2 Coupled CFD-CSM model for the F/A-18 wing.

For the communication with the B2000++ FEM solver, a library has been implemented whose purpose is: to send the coordinates of the wetted surface nodes, to communicate the current time increment size, and to send the integrated nodal forces to the B2000++ FEM solver at each time step. It also receives the interpolated displacements from the FEM solver.

Within the B2000++ FEM solver, the spatial coupling and the MPI communication with the NSMB CFD solver is encapsulated in a natural boundary condition. In the FEM model description, it is sufficient to add the directive "nbc_fsi_nsmb" to the analysis case description. This activates the natural boundary condition which in turn sets up the MPI communication with the NSMB CFD solver.

Since the FEM solver is nonlinear, it is possible for highly nonlinear problems that convergence of the Newton iterations cannot be obtained in a single increment that corresponds to the time increment size as is specified by the CFD solver. In this case, the FEM solver performs several increments with smaller time increment sizes, while ensuring that the sum of them matches the CFD time increment size. When this point is reached, the FEM solver initiates the transfer of the interpolated displacements to the CFD solver.

D. Grid Deformation Tool in NSMB

The remeshing tool implemented in the NSMB CFD solver is a combination of Volume Spline Interpolation and Transfinite Interpolation, see [3] for more details. Volume Spline Interpolation is used to move the prescribed grid points (these are the grid points for which the displacements are known) and to move the block edges. Transfinite Interpolation is then used to generate the grid on the block faces and then to generate the new volume mesh. The time to re-mesh the grid of the F/A-18 fighter having around 50 Million grid points is less than one minute on an HPC cluster.

E. Grid Deformation Tool in FINFLO

The remeshing tool implemented in the FINFLO flow solver is based on linear interpolation inside cells of an auxiliary equally spaced rectangular grid (Fig. 3). The size and the resolution of the grid can be changed. At the first phase all surface displacements from the FEM model are grouped to the auxiliary grid cells according to their locations in the grid. Next the displacements are averaged in all occupied cells. In the third phase the averaged displacements are extrapolated to the surrounding cells and smoothly faded out. In the final step the displacements in the cells are averaged to the nodes of the grid. The averaging is done using eight surrounding cells at each node. Now the computational volume grid, including the solid surface, can be deformed node by node using linear interpolation inside the auxiliary grid cells. The procedure guarantees a continuous deformation, but is lacking the ability to handle correctly differently bend flaps next to each other. An example of FINFLO's deformation tool functioning is seen in Fig. 4.

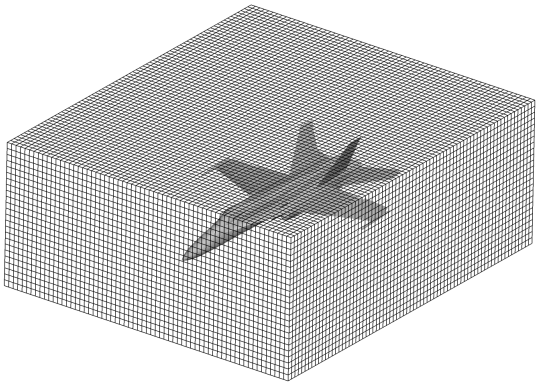

Fig. 3 An auxiliary rectangular deformation grid used in the FINFLO flow solver.

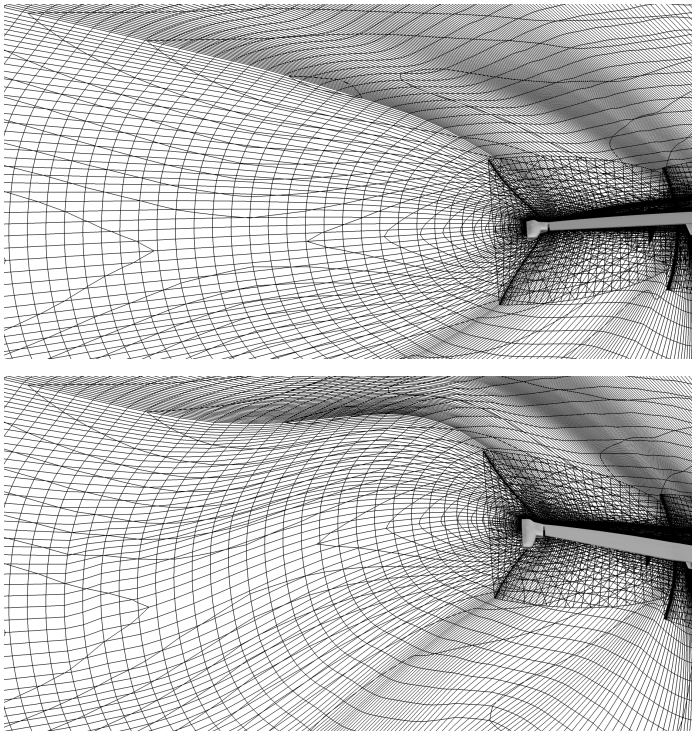

Fig. 4 An undeformed Hornet CFD model volume grid on top and a deformed one below.

IV. Computational Models

To compute the flow solution two different grids were used, one generated in Switzerland and one in Finland. The grid topologies as well as the engine treatment are described in Ref. [2] There are some differences between the grids. The Finnish grid includes the engine channel and the flow nozzle. Boundary conditions are applied on these surfaces to take into account the flow into and out of the engine. The Swiss CFD model does not have an engine, instead considers flow through the engine duct. For the structural part the same FEM model can used and the loads can be transferred from the flow solutions using different grids and flow solvers to the same FEM model.

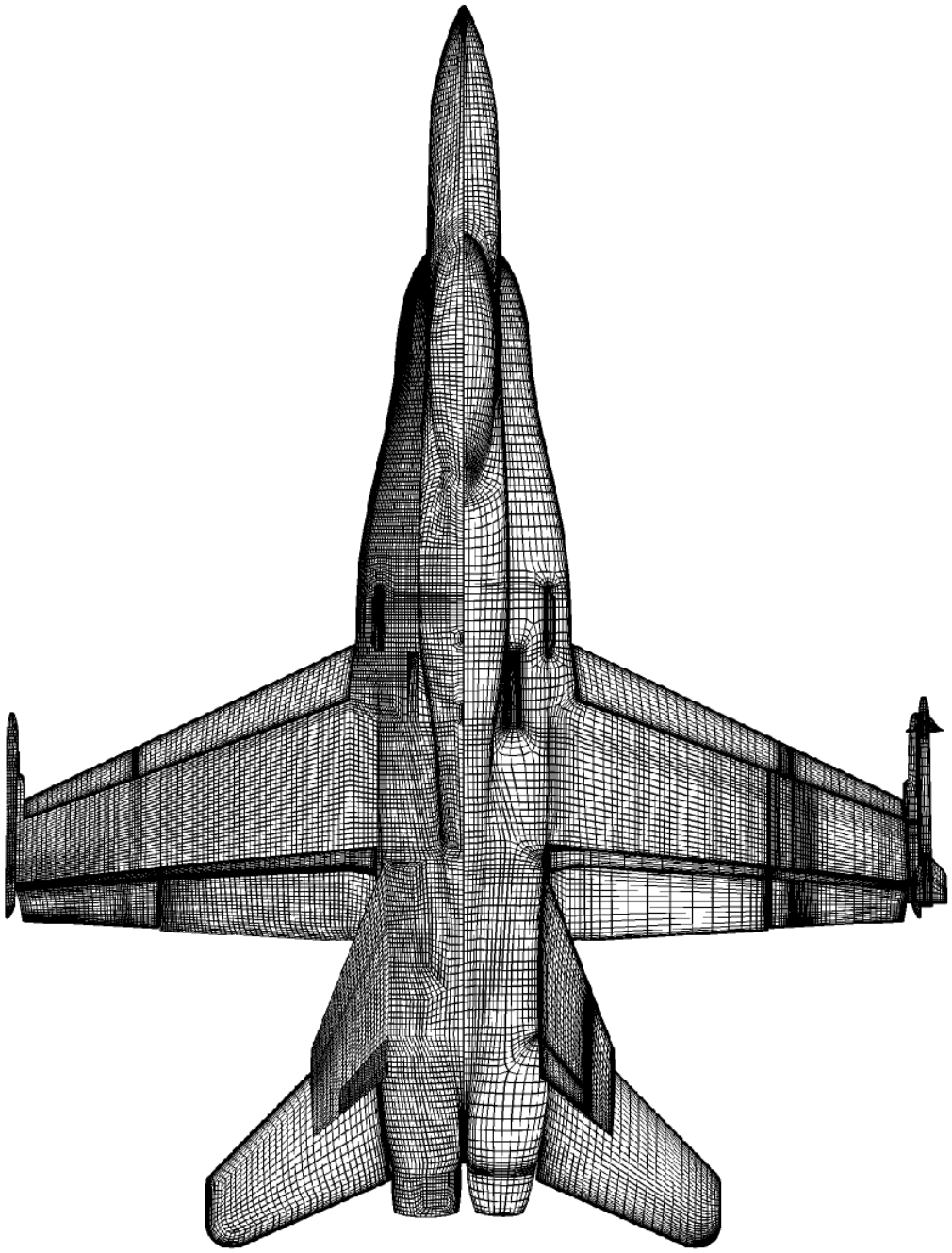

Fig. 5 Surface grid comparison. The Swiss F/A-18C surface grid on the left and the Finnish surface grid with the AIM-9M on the right. (every 2nd grid line shown).

Both grids are multi-block structured ones employing Chimera blocks to allow for flexibility in controlling flap positions and in modeling geometrical details. The Swiss model consists of 40 million cells in 3664 blocks and the Finnish one has around 27 million cells in 89 blocks. The grids have been generated using ICEM CFD and Pointwise software, respectively.

All control surfaces and the wing tip projectile in the Swiss and Finnish grids are modeled using overlapping blocks. The usage of overlapping blocks requires small gaps between the main wing and the control surfaces. On the leading edge side the gap between the wing and the leading edge flaps in both grids is bigger than in real aircraft. On the trailing edge side the gap geometry is more realistic than on the leading edge side. However, in both models the geometry of the gaps around the trailing edge flaps and shrouds is simplified. In the Finnish CFD model the engine effects on the surrounding flow field can be described by defining the flow conditions at locations where the engine would be connected to the model. The engine nozzle shape is adjusted according to the power setting.

The volume grid resolution of the Swiss grid is higher than the resolution of the Finnish grid. The nominal first cell height of the Swiss grid is smaller but the cell height stretching is larger. The radius of the Swiss volume grid is about 250 m while the radius of the Finnish grid is about 500 m. A top view of the grids is shown in Fig. 5. The grids in numbers are presented in Table 1.

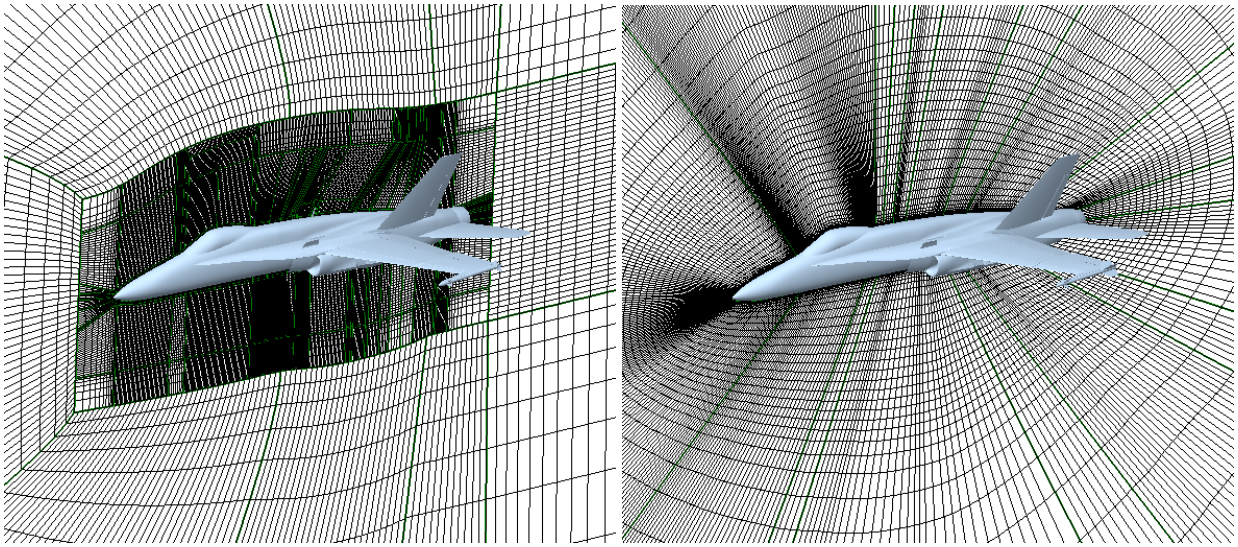

Fig. 6 Comparison of the grids on the symmetry plane.

Table 1 Comparison between the Swiss grid and the Finnish grid (half aircraft). The Finnish grid contains AIM-9M Sidewinder on the wing tip.

Case W035	Swiss	Finnish
NOF cells	39 967 936	27 571 200
NOF surface elements	292 304	284 096
NOF blocks	3664	89

A. FEM

The FEM model used in the study here was presented in detail in [3]. The Nastran BDF file of the F/A-18 FEM model was converted to the B2000++ format using an automatic conversion tool. This tool also changed the formats from the imperial system to SI units. Several singularities in the FEM model were identified and replaced. The FEM model is rather coarse near the wing tip and does not fully cover the wetted surface. This initially led to oscillations in the geometry when performing an FSI calculation. This was corrected by adding several grid points to the SIWA and launcher that were connected by means of rigid-body elements to the structure.

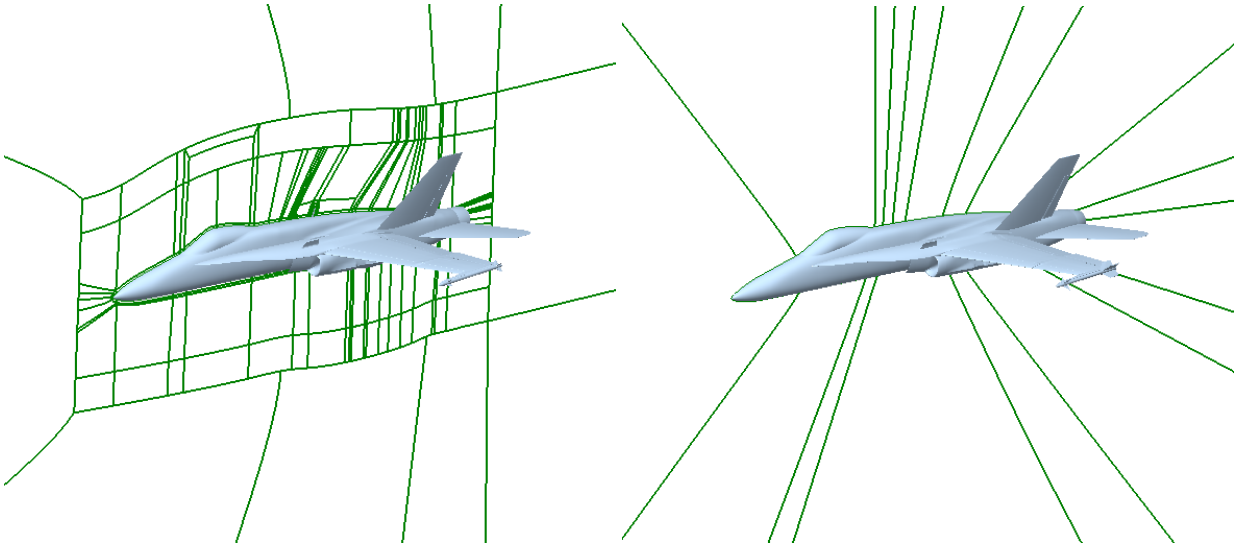

Fig. 7 Grid topology on the symmetry plane.

The Finnish global FE model of FINAF F/A-18 Hornet was developed at Patria by 2005. The model of the whole aircraft contains about 1.5 million DOFs and is applied within MSC Nastran 2012 [5]. The control surfaces can be set at desired deflections held in place with stiff rods modelling the actuators. A semi-automatic procedure is available for transferring the FINFLO-based load distributions onto the FE model. Like the Swiss model, the Finnish FE model is rather coarse in the wing tip area and does not cover the tip missile or its launcher. For these components, the aerodynamic loads are added as point forces and moments. The surface deformations resulting from linear Nastran analyses are transferred back to the CFD grid via a Patran-based procedure.

V. Results

The flight conditions were selected in order to get a sufficiently large deformation on the wing. The case corresponds to a design load case for a wing (W035), which is a steady-state pull-up at $Ma \approx 0.85$. See Table 2 for a summary of the free stream conditions. The flap angles were obtained from a flight-mechanics simulation.

Simulations were performed using two codes with and without the FSI, two grids and two turbulence closures. Only a few results will be given here. The lift and drag coefficients as calculated using several computational options are given in Table 2.

Table 2 F/A-18 simulation conditions.

Altitude	0	ft
Mach	0.849	
Load factor	7.5	
p_∞	101325	Pa
ρ_∞	1.225	kg/m^3
T_∞	288.15	K
Re/meter	$1.98 \cdot 10^7$	$1/m$
α	5.53	deg

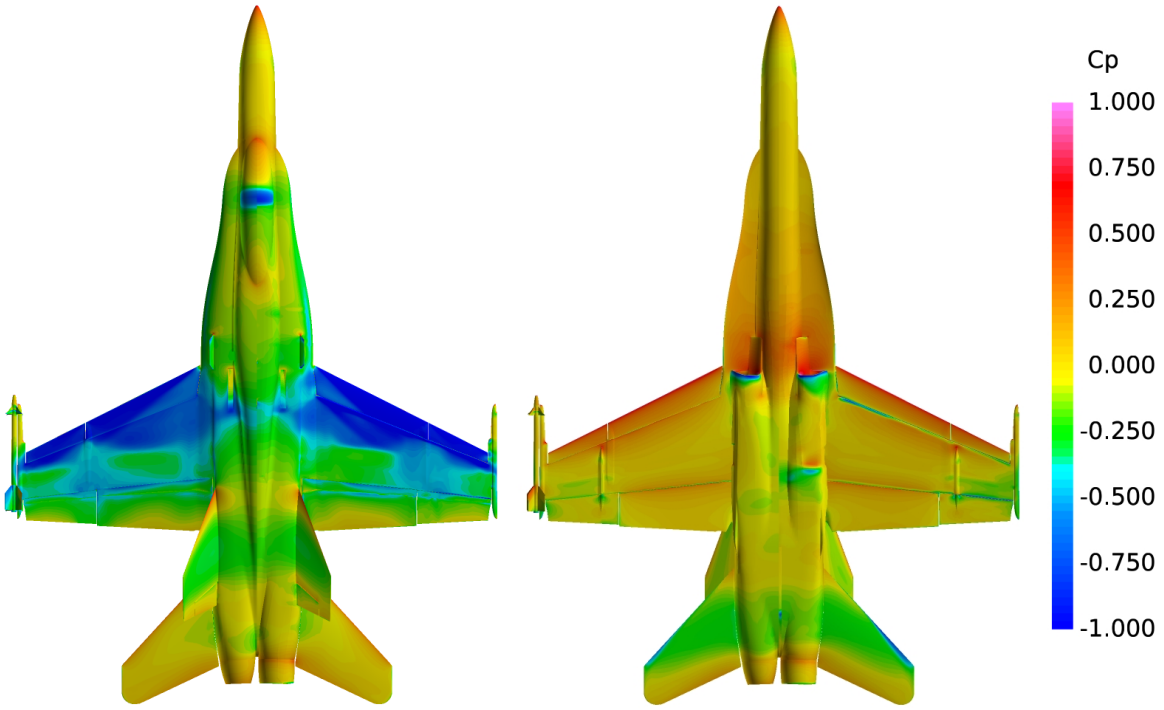

Fig. 8 Surface pressure coefficient distributions obtained using the FINFLO flow solver and the Swiss and Finnish grids. The Finnish grid solution is on the left sides containing an AIM-9M.

Table 3 F/A-18 simulated lift and drag coefficients.

	NSMB		FINFLO	
Coefficient	SST	SA	SST	SA
C_L	0.5230	0.5033	0.5156	0.5132
C_D	0.0623	0.0653	0.0909	0.0913

A. Comparison of the results on the undeformed grids

The effect of different grids and turbulence models was studied by simulating the flow fields using the FINFLO code. Surface pressure coefficient distributions are shown in Fig. 8 using both grids. The Swiss grid is on the right-hand side in the figure. The plotted result is from the second-densest grid level applying the SST $k-\omega$ turbulence model. It is seen that the Swiss grid produces a bit more details inside the low-pressure area compared to the Finnish grid. Owing to the coarse grid density, the shock structure is vague and in a different location compared to the results obtained with the dense grid. On the lower surface the results are practically the same and the differences are caused by the differences in the surface geometries. In the Swiss-grid results there is an over pressure region in front of the engine inlet.

On the dense grid level the corresponding results using both codes and two turbulence models are shown in Fig. 9. The pressure distributions clearly differ from those obtained with the coarse grid. The pressure distributions simulated by the SST- and SA-models are very similar and it can be concluded that in this case the choice between these turbulence models plays a minor role. In the Swiss result the influence of the turbulence model is more visible on the wing surface. The same behaviour can be concluded on the basis of the calculated force coefficients by NSMB and FINFLO in Table 3. In the results of the table, the grids and the codes used are different. In that respect the Swiss and Finnish results can be considered to be close enough each others. The drag coefficients cannot be compared between the countries, because the engine modeling affects the drag more than the lift force.

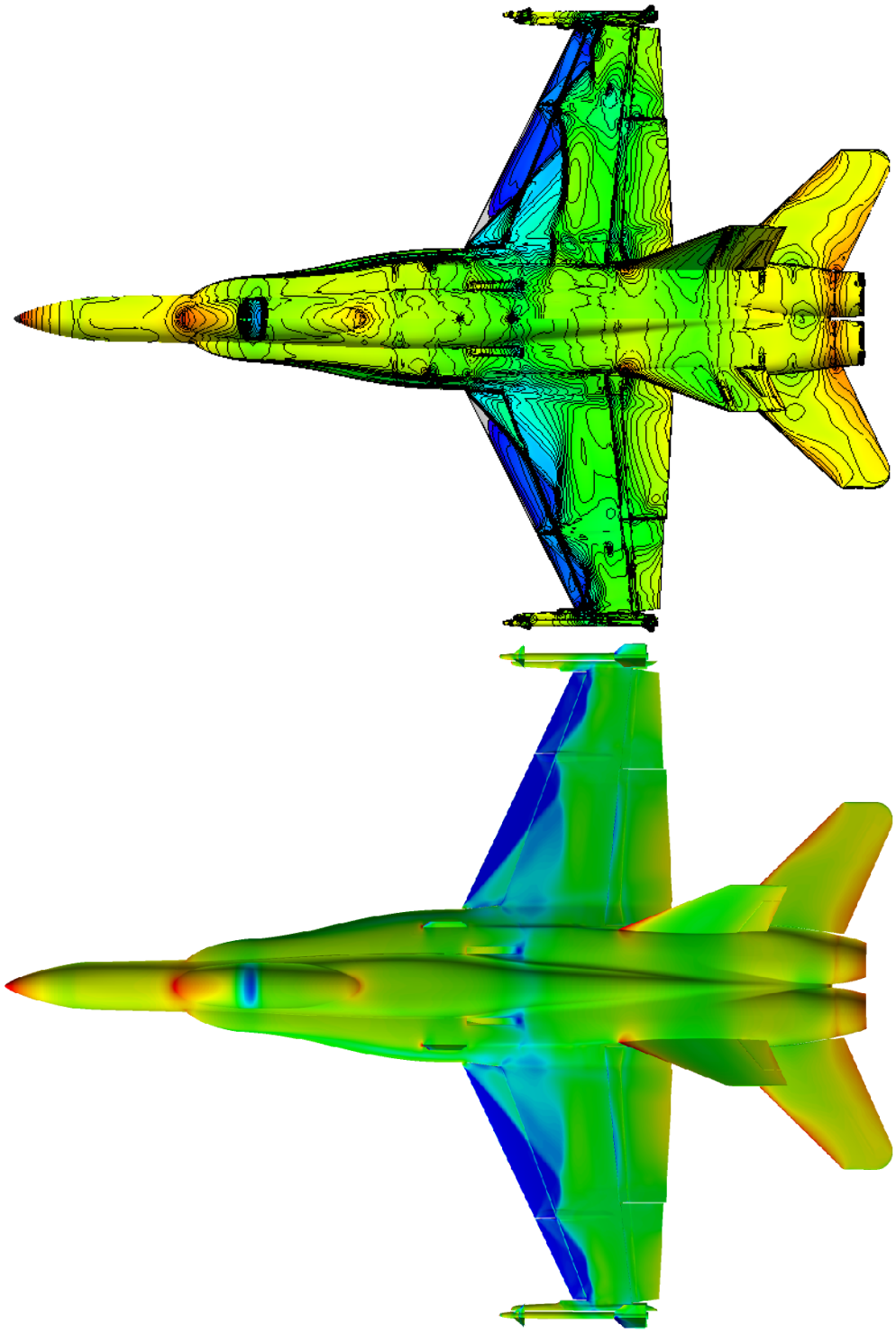

Fig. 9 Surface pressure coefficient distributions obtained using NSMB and FINFLO (undeformed geometries) and different turbulence closures. The SST model on the right-hand side, the Spalart-Allmaras model on the left-hand side of the plane.

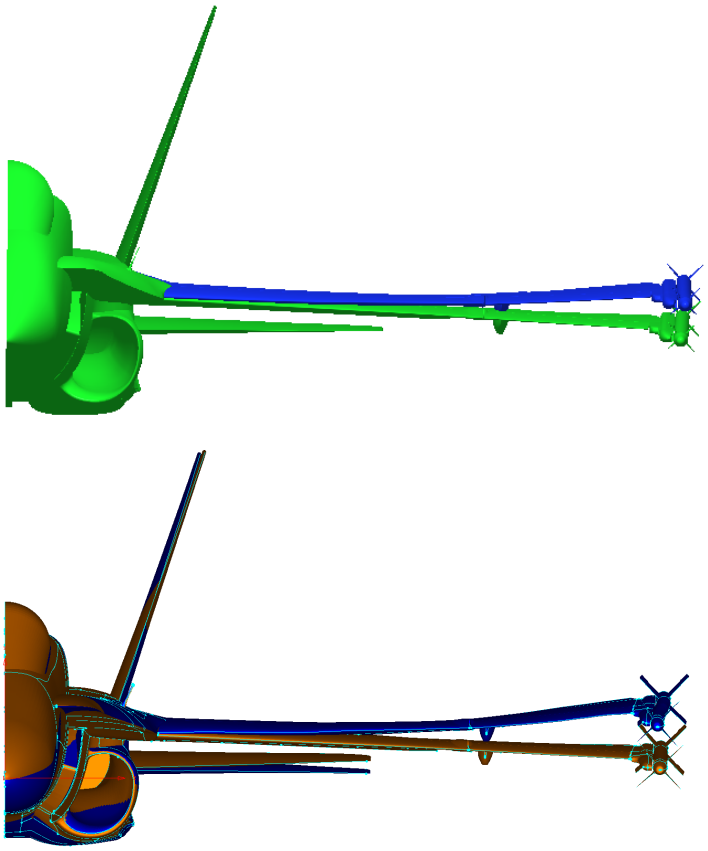

Fig. 10 Deformed and undeformed geometries as calculated by NSMB-B2000++ coupling (on the top) and the FINFLO-Nastran coupling (at the bottom).

B. Simulations on the deformed grids

FSI results are given for the SST $k-\omega$ model. Eight FSI cycles were used for the FINFLO-Nastran simulation. At the beginning under-relaxation was applied for displacements. After the third cycle, no-under-relaxation was needed. The final deformed wing can be seen in Fig. 10. The corresponding pressure distributions are given in Fig. 11. In spite of the fact that the wing tip moves about 0.4 m there are only small differences in the pressure distributions on the wing and the horizontal tail. This indicates that there is only a small twist in the wing.

The NSMB-B2000++ simulations employed 5 FSI cycles; every 300 steps the deformation of the wing was computed and the mesh was regenerated. No under-relaxation was needed. The convergence of the deformation process was faster when using the Spalart-Allmaras turbulence model.

Table 4 F/A-18 calculated loads [kN].

Method	Half a plane	Wing with a missile
FINFLO undeformed	537.11	402.15
FINFLO deformed	519.96	363.43
NSMB undeformed	500.3	
NSMB deformed	429.7	
Boeing data [28, 29]	517.75	384.74

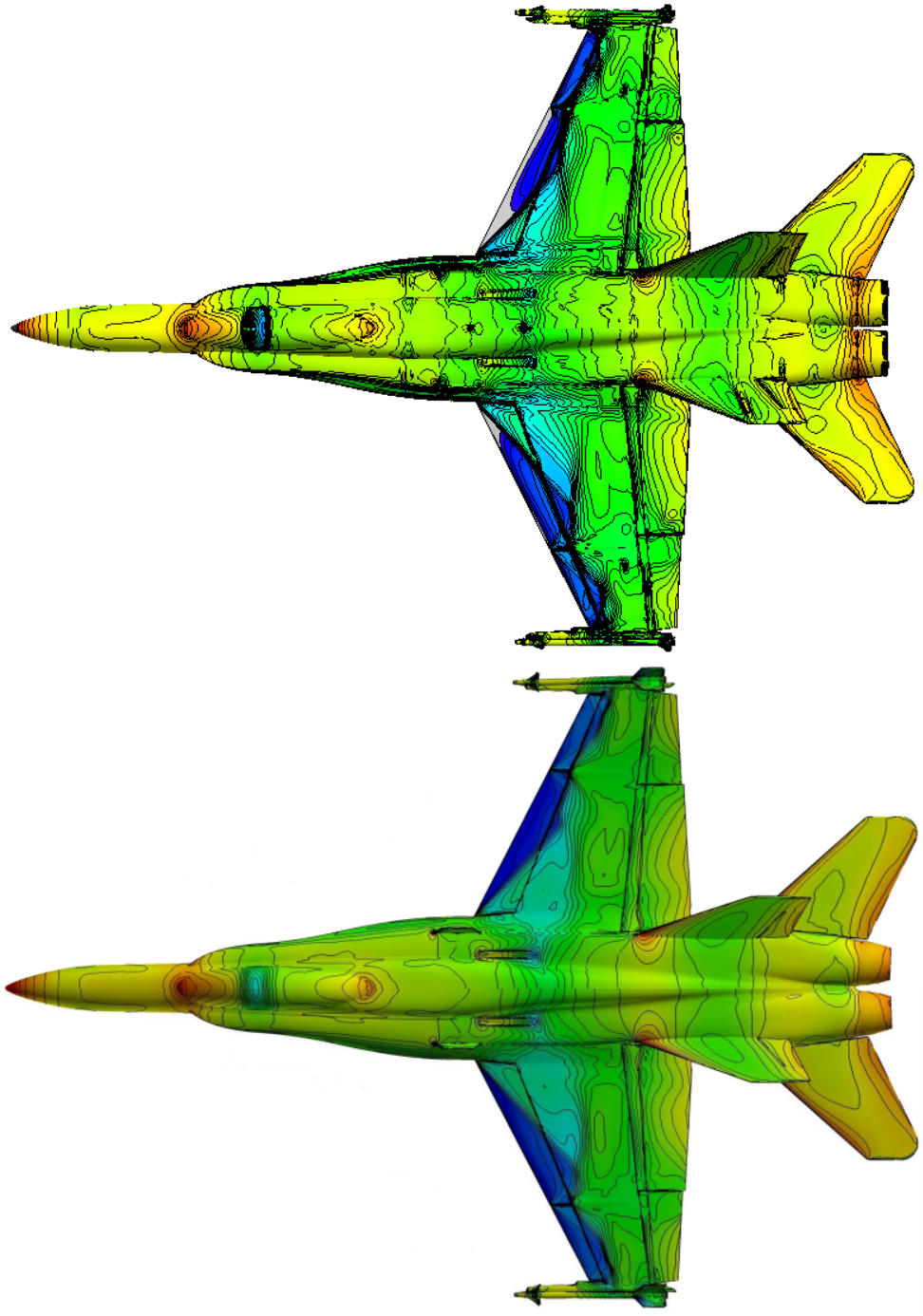

Fig. 11 Pessure coefficient distributions obtained using the Swiss grid and the NSMB-B2000++ coupling (top) and FINFLO-Nastran coupling (below). The deformed geometry is on the right-hand side of the plane and the rigid one on the left-hand side.

The calculated loads are compared with the Boeing design loads for W035 [28, 29] in Table 4. It is seen that the calculated load on the wing as simulated by FINFLO is about 10 % higher in a case of the undeformed wing. In the case of the total force the difference is smaller indicating that the force on the other parts increases in the case of the deformed configuration. For NSMB the total load varies by about 16 % between the cases.

VI. Conclusions

CFD simulations were made in Finland and Switzerland to better understand the influence of the flow solver, turbulence model, the CFD grid and size and the FEM model on the structural deformation. Both CFD solvers employ multi-block structured grids, and use the chimera methods to simplify the mesh generation for complex geometries and to handle control surface deflections of aircraft.

On the undeformed grids computed lift coefficients are in good agreement, and the flow solutions are comparable. It is not possible to compare the drag coefficients due to differences in engine modeling, but the lift coefficients predicted by different codes and grids are within two per cent. The difference between the turbulence models in minimal in the Finnish solution, whereas a larger deviation exists in the Swiss results. In spite of the differences, the results can be considered to be very satisfactory, since no tuning was made in computational parameters and both countries applied their own best-practice procedures in their simulations.

On the deformed grid there are more differences. These are probably caused by the different structural models. The wing deformation is milder in the Swiss approach, whereas in the case of the Finnish model the deformation is about 20 % larger. The deformation does not seemingly affect on the pressure distribution, but on the total force on the wing the effect is about 10 % and 16 % with FINFLO and NSMB, respectively.

Taking into account the structural deformation in the simulation needs more consideration in the future studies. There are clear differences in the results that are not caused by the flow solvers, since with the rigid plane the results are practically the same. The FEM solvers are very well verified, thus the difference is caused by the FEM model or the transfer of loads. In the present steady-state simulation the FSI affects the results by about ten per cent, but it is important to verify the models for more severe asymmetric or time-dependent cases.

References

[1] Vos, J., Rizzi, A., Corjon, A., Chaput, E., and Soinne, E., "Recent advances in aerodynamics inside the NSMB (Navier Stokes multi block) consortium," *36th AIAA Aerospace Sciences Meeting and Exhibit*, 1998, p. 225. AIAA Paper 1998–0025.

[2] Guillaume, M., Gehri, A., Stephani, P., Vos, J., Siikonen, T., Salminen, E., and Mandanis, G., "Swiss/Finnish Computational Fluid Dynamics Simulation on the F/A-18," *Proceedings of the 28th ICAS Congress*, Brisbane, 2012, pp. 1–6. ICAS Paper 2012-10.6.1.

[3] Vos, J. B., Charbonnier, D., Ludwig, T., Merazzi, S., Gehri, A., and Stephani, P., "Recent Developments on Fluid Structure Interaction Using the Navier Stokes Multi Block (NSMB) CFD Solver," *35th AIAA Applied Aerodynamics Conference*, 2017, p. 4458. AIAA Paper 2017–4458.

[4] "B2000++," `http://www.smr.ch/products/b2000/`, 2018. Accessed: May 9th, 2018.

[5] "MSC Nastran," `http://www.mscsoftware.com/product/msc-nastran`, 2018. Accessed: May 15th, 2018.

[6] Guillaume, M., Vos, J., Stephani, P., Gehri, A., Mandanis, G., and Mandanis, G., "Fluid structure interaction simulation on the F/A-18 vertical tail," *40th Fluid Dynamics Conference and Exhibit*, Chicago, 2010, p. 4613. AIAA Paper 2010–4613.

[7] Vos, J. B., Sanchi, S., and Gehri, A., "Drag Prediction Workshop 4 Results Using Different Grids Including Near-Field/Far-Field Drag Analysis," *Journal of Aircraft*, Vol. 50, No. 5, 2013, pp. 1615–1627.

[8] Vos, J., Bourgoing, A., Soler, J., and Rey, B., "Earth re-entry capsule CFD simulations taking into account surface roughness and mass injection at the wall," *International Journal of Aerodynamics*, Vol. 5, No. 1, 2015, pp. 1–33.

[9] Pena, D., Hoarau, Y., and Laurendeau, É., "Development of a three-dimensional icing simulation code in the NSMB flow solver," *International Journal of Engineering Systems Modelling and Simulation*, Vol. 8, No. 2, 2016, pp. 86–98.

[10] Grossi, F., Braza, M., and Hoarau, Y., "Prediction of transonic buffet by delayed detached-eddy simulation," *AIAA Journal*, Vol. 52, No. 10, 2014, pp. 2300–2312.

[11] Shinde, V., Marcel, T., Hoarau, Y., Deloze, T., Harran, G., Baj, F., Cardolaccia, J., Magnaud, J.-P., Longatte, E., and Braza, M., "Numerical simulation of the fluid–structure interaction in a tube array under cross flow at moderate and high Reynolds number," *Journal of Fluids and Structures*, Vol. 47, 2014, pp. 99–113.

[12] Deloze, T., Hoarau, Y., and Dušek, J., "Transition scenario of a sphere freely falling in a vertical tube," *Journal of Fluid Mechanics*, Vol. 711, 2012, pp. 40–60.

[13] Deloze, T., Hoarau, Y., and Dušek, J., "Chimera method applied to the simulation of a freely falling cylinder in a channel," *European Journal of Computational Mechanics/Revue Européenne de Mécanique Numérique*, Vol. 19, No. 5-7, 2010, pp. 575–590.

[14] Hoarau, Y., Pena, D., Vos, J. B., Charbonier, D., Gehri, A., Braza, M., Deloze, T., and Laurendeau, E., "Recent Developments of the Navier Stokes Multi Block (NSMB) CFD solver." *54th AIAA Aerospace Sciences Meeting*, 2016, p. 2056.

[15] Spalart, P., and Allmaras, S., "A one-equation turbulence model for aerodynamic flows," *30th Aerospace Sciences Meeting & Exhibit, Jan*, 1992, pp. 6–9. AIAA Paper 92-0439.

[16] Langtry, R., and Menter, F., "Transition modeling for general CFD applications in aeronautics," *AIAA paper*, Vol. 522, No. 2005, 2005, p. 14.

[17] Spekreijse, S. P., Prananta, B. B., and Kok, J. C., "A simple, robust and fast algorithm to compute deformations of multi-block structured grids," *NLR-TP-2002-105*, 2002.

[18] Siikonen, T., Rautaheimo, P., and Salminen, E., "Numerical Techniques for Complex Aeronautical Flows," *Proceedings of the ECCOMAS 2000 Conference*, 2000.

[19] Miettinen, A., and Siikonen, T., "Application of pressure- and density-based methods for different flow speeds," *International Journal for Numerical Methods in Fluids*, Vol. 79, No. 5, 2015, pp. 243–267. doi:10.1002/fld.4051, URL `http://dx.doi.org/10.1002/fld.4051`, fld.4051.

[20] Viitanen, V. M., and Siikonen, T., "Numerical simulation of cavitating marine propeller flows," *9th National Conference on Computational Mechanics (MekIT'17)*, Trondheim, Norway, 2017. URL `http://agraficastorres.es/cimnecongress/MEKIT_2017/Ebook%20Mekit17.pdf`, international Center for Numerical Methods in Engineering (CIMNE), pp. 385–409. Trondheim, Norway. ISBN: 978-84-947311-1-2.

[21] Viitanen, V., Hynninen, A., Lübke, L., Klose, R., Tanttari, J., Sipilä, T., and Siikonen, T., "CFD and CHA simulation of underwater noise induced by a marine propeller in two-phase flows," *Fifth International Symposium on Marine Propulsors (smp'17)*, Espoo, Finland, 2017.

[22] Wallin, S., and Johansson, A., "Modelling of streamline curvature effects on turbulence in explicit algebraic Reynolds stress turbulence models," *Second International Symposium on Turbulence and Shear Flow Phenomena*, Stockholm, Sweden, 2001.

[23] Van Albada, G., Van Leer, B., and Roberts, W., "A comparative study of computational methods in cosmic gas dynamics," *Astronomy and Astrophysics*, Vol. 108, No. 76, 1982, pp. 76–84.

[24] Fujii, K., "Numerical Experiment of the Flight Trajectory Simulation by Fluid Dynamics and Flight Dynamics Coupling," *11th AIAA Computational Fluid Dynamics Conference*, Vol. 1, Orlando, FL, 1993, pp. 297–308. AIAA Paper 93–3324–CP.

[25] Yoon, S., and Jameson, A., "Lower-Upper Symmetric-Gauss-Seidel Method for the Euler and Navier–Stokes Equations," *AIAA Journal*, Vol. 26, No. 9, 1988, pp. 1025–1026.

[26] "Langley Research Center, Turbulence Modeling Resource," `http://turbmodels.larc.nasa.gov/sst.html`, 2018. Accessed: December 15th, 2017.

[27] Guillaume, M., Gehri, A., Stephani, P., Vos, J., and Mandanis, G., "F/A-18 vertical tail buffeting calculation using unsteady fluid structure interaction," *The Aeronautical Journal*, Vol. 115, No. 1167, 2011, pp. 285–294.

[28] "F-18 Structural Design Loads Report," Tech. Rep. MDC Report A4930, Volume III, Supplement I, Revision A, McDonnell Aircraft Company, St. Louis, Missouri, USA, 1985.

[29] "F/A-18 Inertia Loads Report," Tech. Rep. MDC Report A4931, Revision A, McDonnell Aircraft Company, St. Louis, Missouri, USA, 1983.